Two mechanisms for inward rectification of current flow through the purinoceptor $P2X_2$ class of ATP-gated channels

Zhen Zhou and Richard I. Hume

Department of Biology, University of Michigan, Natural Science Building, Ann Arbor, MI 48109-1048, USA

(Received 28 August 1997; accepted after revision 17 October 1997)

1. The ATP receptor subunit $P2X_2$ was expressed in *Xenopus* oocytes and human embryonic kidney (HEK) 293 cells. ATP-activated currents were studied with two-electrode voltage clamp recordings from oocytes, whole-cell recordings from HEK 293 cells, and outside-out patch clamp recordings from both cell types. The steady-state current–voltage (*I–V*) relation showed profound inward rectification in all recording configurations.

2. Recordings from outside-out patches demonstrated that inward rectification does not require intracellular Mg^{2+} or polyamines, and that inward rectification was present when the same solution was used on both sides of the patch.

3. Voltage jump experiments were performed to evaluate the voltage dependence of channel gating. After fast voltage jumps, instantaneous current jumps were followed by substantial relaxations to the steady state. The time course of the current relaxations could be fitted by single exponential functions. The instantaneous *I–V* relation was less inwardly rectifying than the steady-state *I–V* relation; however, it was not linear.

4. Single channel recordings indicated that the single channel conductance became smaller when the membrane potential became more positive. This decrease could quantitatively account for inward rectification of the instantaneous *I–V* relation.

5. We conclude that inward rectification of $P2X_2$ is due to two mechanisms: voltage-dependent gating and voltage dependence of the single channel conductance.

P2X receptors are ligand-gated channels which mediate fast excitatory responses to ATP. The P2X class of receptors was originally defined by pharmacological criteria, but in the past few years, cDNAs encoding seven P2X receptor subunits have been cloned (Buell, Collo & Rassendren, 1996). Physiological, pharmacological and molecular studies have demonstrated that P2X receptors have a broad distribution in the central nervous system, the peripheral nervous system and in cardiac, skeletal and smooth muscle cells (Burnstock, 1995). However, the correspondence between particular patterns of gene expression and particular P2X receptor subtypes is not yet well understood. One physiological property that characterizes some, but not all, P2X receptor channels is that they pass inward current more easily than outward current (Brake, Wagenbach & Julius, 1994; Evans *et al.* 1996), a characteristic referred to as inward rectification.

The physiological role of inward rectification in a ligand-gated cation channel has been explored in some detail in neurons expressing neuronal nicotinic acetylcholine receptor (nAChR) channels. In contrast to skeletal muscle nAChR channels, which have a nearly linear current–voltage (*I–V*) relation, most neuronal nAChR channels show pronounced inward rectification (Sargent, 1993). It has been suggested that inward rectification in neuronal nAChR channels is important because the decrease in conductance at more positive membrane potentials acts to prevent shunting of the spike once the threshold is crossed. Because any cation channel with a linear *I–V* relation will tend to shunt the spike, it might be expected that cation channels gated by other transmitters would also show inward rectification, and indeed there are inwardly rectifying cation channels gated by glutamate (Boulter *et al.* 1990) and serotonin (Maricq, Peterson, Brake, Myers & Julius, 1991), as well as acetylcholine and ATP. Our goal for this paper was to characterize in detail the mechanisms that contribute to inward rectification in P2X channels of defined subunit composition, so that we might move towards a molecular understanding of this important physiological mechanism.

The mechanism of inward rectification has been extensively studied in several types of channels. Intrinsic inward rectification has been suggested in a channel formed from aggregation of small peptides (Kienker, DeGrado & Lear, 1994). Muscle nAChR channels show a very small degree of inward rectification because channel gating is weakly voltage dependent (Magleby & Stevens, 1972), and neuronal

nAChR channels show substantial inward rectification due to a combination of open channel block by internal Mg^{2+} and voltage-dependent gating (Ifune & Steinbach, 1990; Sands & Barish, 1992). Intracellular Mg^{2+} is also capable of producing an open channel block of several different inwardly rectifying K^+ channels in excised patches (Matsuda, Saigusa & Irisawa, 1987; Vandenberg, 1987; Davies, McKillen, Stanfield & Standen, 1996). However, Mg^{2+} block cannot account quantitatively for the degree of rectification found in some inwardly rectifying K^+ channels. Soon after Lopatin, Makhina & Nichols (1994) demonstrated that intracellular polyamines are potent blockers of one class of inwardly rectifying K^+ channels, several different groups showed that polyamines can also block several other inwardly rectifying K^+ channels (Ficker, Taglialatela, Wible, Henley & Brown, 1994; Fakler, Brandle, Glowatzki, Weidemann, Zenner & Ruppersberg, 1995), and that polyamines probably are responsible for inward rectification of α-amino-3-hydroxy-5-methylisoxazole-4-propionate (AMPA) class glutamate receptor channels (Kamboj, Swanson & Cull-Candy, 1995; Koh, Burnashev & Jonas, 1995; Bowie & Mayer, 1995).

An important question raised by the work on AMPA receptors was whether block by intracellular polyamines might be the cause of inward rectification of other classes of ligand-gated cation channels as well. We decided to focus our efforts on ATP receptor channels formed by $P2X_2$ subunits because previous work had suggested that there is inward rectification in the *I–V* relation of these channels (Brake *et al.* 1994; Evans *et al.* 1996) and because it has been reported that the amount of inward rectification varies widely among cells expressing $P2X_2$ (Evans *et al.* 1996), as might be expected if the concentration of polyamines varies between cells. Our results indicate that polyamines play no role in inward rectification of this class of ATP receptors, but that inward rectification can be accounted for by a combination of voltage-dependent gating and voltage dependence of the single channel conductance.

METHODS

Electrophysiological recordings of $P2X_2$ expressed in *Xenopus* oocytes

Female *Xenopus laevis* were purchased from Xenopus 1 (Ann Arbor, MI, USA). Oocytes were harvested by procedures approved by the University of Michigan Committee on the Use and Care of Vertebrate Animals. Frogs were anaesthetized by immersion in well water containing 3-aminobenzoic acid ethyl ester (1 g l^{-1}; Sigma). A frog was considered to be fully anaesthetized when the nose flare and swallow reflexes were absent. A small vertical incision in the lower half of the abdomen was made, which allowed a lobe of the ovary to be exposed. Prior to removing a portion of the ovarian lobe, a loop of suture was tied to prevent bleeding, and then tissue distal to the ligature was removed with scissors. The muscle layer and the skin layer of the incision were sutured separately and the frog was allowed to recover in well water without anaesthetic. Usually, it took about half an hour for full recovery. Frogs were observed daily for signs of infection, but no infection was apparent in any frog used, and so no antibiotics were administered.

The excised lobe was separated mechanically into small clusters of oocytes with fine forceps and the clusters were treated with collagenase (Worthington) to obtain well-separated oocytes. *Xenopus* oocytes (stage V–VI) were injected with $P2X_2$ RNA (typically 50 ng per oocyte, although 2·5 ng per oocyte was usually used when we wanted to make single channel recordings) synthesized *in vitro* from cloned cDNA (the $P2X_2$ plasmid was obtained from Dr D. Julius, University of California, San Francisco, USA) using the T7 message machine kit (Ambion). Two days later, oocytes were screened for responses to 50 μM ATP using two-electrode voltage clamp. Oocytes with high expression levels (>1000 nA) were used for patch clamp recordings. Two-electrode voltage clamp (with an Axoclamp-2A) and patch clamp recordings (with a Dagan 3900) were made using standard methods. In all the experiments on intact oocytes and on patches pulled from oocytes ATP was applied by perfusing the recording chamber. Solution exchange in the oocyte chamber occurred with a time constant of about 4 s. The standard external solution contained (mM): 90 NaCl, 1 KCl, 1·7 $MgCl_2$, 1·7 $CoCl_2$ and 10 Hepes (pH 7·4). The pipette solution for two-electrode voltage clamp contained 3 M KCl and 0·4 M EGTA. The standard internal solution for outside-out patch clamp experiments contained (mM): 70 KF, 20 KCl, 10 Hepes, 10 K_2EGTA and 5 EDTA (pH 7·4). The external and internal solutions for patch clamp recordings were varied in some experiments, as indicated in Results.

Prior to patch clamp recordings, a hypertonic solution containing (mM): 250 choline chloride, 20 KCl, 10 K_2EGTA, 1 $MgCl_2$ and 10 Hepes (pH 7·4) (modified from the solution used by Methfessel, Witzemann, Takahashi, Mishina, Numa & Sakmann, 1986), was used to shrink oocytes in order to allow removal of the vitelline layer with fine forceps. For patch clamp recordings, pipettes were coated with Sylgard® and polished to have resistances between 2 and 5 MΩ.

Electrophysiological recordings of $P2X_2$ expressed in human embryonic kidney (HEK) 293 cells

HEK 293 cells were cultured in minimum essential medium (MEM) supplemented with 10% fetal bovine serum, penicillin–streptomycin solution (5000 units penicillin and 5 mg streptomycin per 100 ml) and conalbumin (0·04 mg ml^{-1}). $P2X_2$ was co-transfected into HEK 293 cells with a plasmid encoding the S65T mutant form of green fluorescent proteins (GFP; Clontech no. 6088-1) by a calcium phosphate precipitation protocol (Chen & Okayama, 1987). Each 60 mm culture dish received 2·5 μg $P2X_2$ plasmid and 1 μg GFP plasmid. One day after transfection, the cells were replated on polyornithine coated 35 mm dishes. Electrophysiological recordings were made on GFP-positive cells 1–5 days after replating. Patch clamp recordings were made using standard methods (with an Axopatch 200). The standard external solution contained (mM): 132 NaCl, 5·3 KCl, 1·3 NaH_2PO_4, 1·7 $MgSO_4$, 5·4 $CaCl_2$, 12 Hepes, 6·3 glucose and 0·3 Phenol Red (pH 7·4), and the standard internal solution contained (mM): 135 CsCl, 2 $MgCl_2$, 1 EGTA, 10 Hepes and 10 glucose (pH 7·4). The external and internal solutions were varied in some experiments, as indicated in Results. In studies of HEK 293 cells, ATP was applied by positive pressure applied to the back of pipettes with a tip diameters of 2–5 μm that were placed approximately 100 μm from the cell or patch. The duration of ATP application was controlled by a solenoid valve, or for long applications, by simply removing the pipette from the bath.

Data acquisition and analysis

The steady-state *I–V* relation was determined by using both voltage jumps (step protocol) and voltage ramps. The step protocol

was also used to obtain the instantaneous *I–V* relation. In the step protocol, the membrane potential was held at −100 mV, and then stepped to other potentials for a duration that was sufficient for the currents to relax to steady state (for patches at least 40 ms, see Fig. 2). Step protocols with an ascending series of steps gave *I–V* relations that were indistinguishable from protocols with a descending series of steps. In the ramp protocol, membrane potential was ramped from −100 to +100 mV, or from +100 to −100 mV over either 2 s (recordings from intact oocytes), or 200 ms (whole-cell recordings from HEK 293 cells and recordings from outside-out patches). In all cases, the *I–V* relation of the ATP-activated current was determined by subtracting the response of the cell or patch in the absence of ATP from that in the presence of ATP. Control experiments which demonstrated that the rate of the ramp depolarizations was sufficiently slow to give a good approximation of the steady-state *I–V* relation are presented in Results.

When data were obtained from a series of cells or patches, the results were expressed as means ± S.E.M., n indicates the number of patches/cells. In several figures the error bars (S.E.M.) are not visible because they are smaller than the symbols used. Student's t test was used to determine whether population means differed, with significance taken to be $P < 0{\cdot}05$.

Single channel recordings from oocytes

In most single channel recording experiments a solution containing (mM): 150 NaCl, 1 $MgCl_2$, 10 Hepes and 10 EGTA (pH 7·4) was used as both external and internal recording solution. Single channel amplitude at negative potentials was obtained by holding the membrane potential of outside-out patches at −150, −120, −100, −80, −60 or −40 mV and then recording the current responses in the presence and absence of a concentration of ATP which produced well-separated single channel openings (typically 500 nM or 1 μM ATP). Two hundred traces (25 ms trace^{-1}) were recorded for each trial by Fetchex (Axon Instruments). The amplitude of the unitary current at each potential was estimated from all points histograms that were fitted by the sum of two Gaussian functions (see legend to Fig. 4). Single channel conductance was calculated using the equation $\gamma = i/(V_m - E_{rev})$, where i is the single channel amplitude, V_m is the membrane potential and E_{rev} is the reversal potential which under this recording condition was 0 mV.

We had difficulty obtaining outside-out patches that were stable when maintained at positive membrane potentials for more than a few seconds. Therefore, to get single channel currents at positive membrane potentials, we gave 200 ms ramp depolarizations from –100 to +100 mV in the presence and absence of 500 nM or 1 μM ATP. The criteria used to accept data for analysis are described in Results. The amplitude of single channel currents at different membrane potentials was measured with a cursor from current traces in which the leakage current in the absence of ATP had been subtracted. Single channel conductances were calculated using the equation described above.

RESULTS

The steady-state *I–V* relation of P2X$_2$ showed strong inward rectification

In oocytes expressing P2X$_2$, the steady-state *I–V* relation in response to 50 μM ATP was determined using step depolarizations and ascending 2 s ramp depolarizations. The response of oocytes to ATP was characterized by a large inward current when the membrane potential was negative to the reversal potential and a small outward current when the membrane potential was positive to the reversal potential (Fig. 1*A*). The reversal potential under these recording conditions was −9·4 ± 0·7 mV ($n = 8$), and the rate of desensitization was so slow (time constant, 76 s) that compensation for desensitization during the 2 s of the ramp produced a negligible change in the shape of the *I–V* relation. Figure 1*A* also demonstrates that the step protocol gave the same steady-state *I–V* relation as the ramp protocol. Because the data could be collected more rapidly with the ramp protocol, the majority of the steady-state *I–V* relations reported in this paper used the ramp protocol.

A useful way to characterize the degree of inward rectification in the *I–V* relation is to calculate a rectification index, by taking the ratio of the chord conductances at potentials equal distances positive and negative to the reversal potential. In previous work on P2X$_2$, Evans *et al.* (1996) chose to use the conductance at potentials 50 mV positive and negative to the reversal potential (a potential range of 100 mV) to calculate their rectification index. In our experiments on oocytes expressing P2X$_2$, the ratio of conductances 50 mV positive and negative to the reversal potential was 0·36 ± 0·01 ($n = 8$). However, in all the *I–V* relations shown in Fig. 1, it is apparent that steady-state chord conductance gradually decreased as cells were depolarized from −100 to 100 mV (see also Fig. 3*B*). Therefore, selection of a potential range larger than 100 mV will yield a smaller rectification index, and selection of a potential range smaller than 100 mV will yield a larger rectification index. For instance, for this same set of oocytes, the rectification index calculated from conductances 80 mV positive and negative to the reversal potential was 0·20 ± 0·01 ($n = 8$). In studies of other ligand-gated channels that show inward rectification, such as AMPA class glutamate receptors (Bowie & Mayer, 1995; Koh *et al.* 1995) and neuronal nicotinic acetylcholine receptors (Ifune & Steinbach, 1990), the voltage dependence of rectification has been studied over a wider range than examined by Evans *et al.* (1996). To facilitate comparison with these other channel types, for the rest of this paper we use the ratio of conductances 80 mV positive and negative to the reversal potential as our rectification index.

Xenopus oocytes are known sometimes to glycosylate proteins differently from mammalian cells (Geetha-Habib, Park & Lennarz, 1990), so it was important to test whether the physiological properties of P2X$_2$ channels were dependent on the expression system. We therefore studied P2X$_2$ channels expressed in a human cell line, HEK 293 cells. In HEK 293 cells transfected with P2X$_2$, the steady-state *I–V* relation, determined by whole-cell patch clamp recording with our standard HEK 293 cell external solution and standard Cs-rich internal solution, also showed strong inward rectification (rectification index, 0·15 ± 0·02; $n = 10$).

Known open channel blockers do not cause inward rectification

For an inwardly rectifying cation channel, rectification could be caused by positively charged channel blockers acting from the inside of the cell or negatively charged channel blockers acting from the outside (Hille, 1992). One approach to test for open channel block by impermeant intracellular ions is to study channels in the outside-out patch configuration, where the composition of the solutions bathing both sides of the membrane can be controlled. If inward rectification were due to block by an intracellular cation, then the *I–V* relation would lose its inward rectification soon after the patch was excised if the internal solution did not contain the blocker, and rectification would be maintained if the blocker was added to the internal solution. Evans *et al.* (1996) had previously suggested that

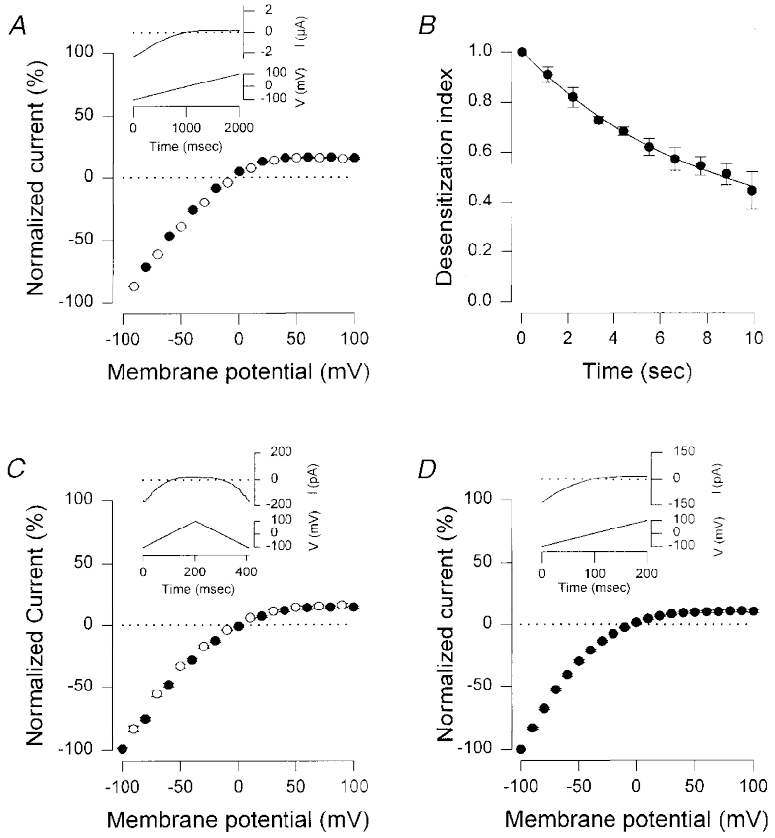

Figure 1. $P2X_2$ receptor currents show profound inward rectification

A, steady-state *I–V* relation of $P2X_2$ activated currents expressed in *Xenopus* oocytes. Oocytes were studied using a two-electrode voltage clamp. The *I–V* relation was determined from the response of oocytes in the presence and absence of 50 μM ATP to step depolarizations from −100 to +100 mV in 20 mV increments (●) and from 2 s ramp depolarizations from −100 to +100 mV (○). Current at each membrane potential is normalized to the current at −100 mV. Data from 8 oocytes are averaged. The inset shows the response of a typical cell (top) to the ramp depolarization (bottom). *B*, desensitization of the current responses to continuous application of 50 μM ATP in outside-out patches excised from oocytes expressing $P2X_2$. Data shown are the means from 4 patches. Time 0 was the time when the response to ATP reached the peak. Current was measured every 1 s after time 0. The desensitization index was defined as the ratio of the current at each time point to the current at time 0. The continuous line is a single exponential fit to the data, which gave a time constant of desensitization of 7·8 s. The curve fit also indicated that desensitization does not decrease current to 0; rather in the steady state 26% of the maximum current remains. *C*, *I–V* relation of outside-out patches excised from oocytes expressing $P2X_2$. *I–V* relations were determined by a sawtooth ramp protocol, which had a 200 ms upward voltage ramp (●) from −100 to +100 mV followed by a 200 ms downward voltage ramp (○) from +100 to −100 mV. These experiments used the standard internal solution for patch clamp recordings which was Mg^{2+} and polyamine free. Current at each membrane potential is normalized to the current at −100 mV. Values are means from 6 patches. The inset shows the response of a typical patch (top) to the sawtooth stimulus (bottom). *D*, internal spermine had no effect on the *I–V* relation. Spermine (100 μM) was included in the standard internal solution and the *I–V* relation was determined by 200 ms ramps from −100 to +100 mV. Values are means from 10 patches. The inset shows the response of a typical patch (top) under these conditions (bottom).

rectification was unlikely to be caused by an intracellular blocker, because prolonged dialysis during whole-cell recording did not lead to changes in rectification. However, dialysis of polyamines from intact cells by whole-cell recording is very slow even in cells much smaller than HEK 293 cells (Kamboj *et al.* 1995) and so block by internal polyamines remained a possibility that needed to be tested more directly.

Most patches excised from oocytes injected with 50 ng of RNA gave responses to 50 μM ATP of more than -100 pA at -100 mV. We therefore were able to obtain data for constructing macroscopic *I–V* relations without having to average records. However, a complication in experiments using outside-out patches is that the responses to 50 μM ATP observed in outside-out patches desensitized much more rapidly (time constant, 7·8 s; Fig. 1*B*) than the responses of intact oocytes (time constant, >1 min). We dealt with desensitization in two different ways. When we used the ramp protocol, it was not necessary to make a correction for the effect of desensitization, because over the 200 ms duration of the ramps, desensitization was expected to decrease the response amplitude by only 2%, which was within the experimental error of our measurements. The use of such rapid ramps raised a different concern, for it was possible that they would no longer reflect the steady-state *I–V* relation. However, Fig. 1*C* shows that responses to the upward and downward going limbs of a sawtooth stimulus were no different, indicating that these experiments indeed produce a steady-state *I–V* relation. The approach used to correct for the effect of desensitization in experiments using the step protocol is described below.

Figure 1*C* also demonstrates, contrary to the predictions of the intracellular blocker mechanism, that the *I–V* relation continued to show strong inward rectification when patches were excised into a simple salt solution without polyamines or magnesium. For a series of patches, some held as long as 2 h, the rectification index was 0·15 ± 0·01 ($n = 14$). To test further whether intracellular positive charged particles are capable of causing inward rectification of P2X$_2$, we added Mg^{2+} or a polyamine to the internal solution bathing excised patches, because of their role in blocking other classes of channels. For polyamines we chose to use either 100 μM spermine, 1 mM spermidine or 10 mM putrescine, because these concentrations are approximately 10 times the IC_{50} for these compounds on AMPA receptor channels (Bowie & Mayer, 1995) and IRK1 channels (Lopatin *et al.* 1994) and therefore would be likely to produce potent block if they were involved in causing rectification in P2X$_2$ channels. The degree of inward rectification in the *I–V* relation of patches excised from oocytes expressing P2X$_2$ was unchanged by the addition of spermine (Fig. 1*D*), spermidine, putrescine or 2 mM Mg^{2+} (respective rectification indices: 0·15 ± 0·01, $n = 10$; 0·22 ± 0·03, $n = 5$; 0·20 ± 0·02, $n = 4$; 0·17 ± 0·02, $n = 5$). The remaining positively charged ion in our standard oocyte internal solution was K^+ and the reversal potential of ATP responses indicated that K^+ was permeant. In addition, substitution of internal K^+ with Na^+ did not change the degree of inward rectification (see below).

Extracellular negatively charged particles could also potentially block channels from the outside at positive membrane potentials, and thereby cause inward rectification. The two major negatively charged particles in our standard oocyte external solution were Hepes and Cl^-. To test the role of these anions on rectification of P2X$_2$ channels, we made recordings from outside-out patches bathed with modified external solutions. Replacement of Hepes in the standard external solution with Tris, a positively charged pH buffer, did not change the inward rectification of patches pulled from oocytes expressing P2X$_2$ (rectification index, 0·07 ± 0·01; $n = 6$). Similarly, substitution of Cl^- by the larger anion $CH_3SO_3^-$ also did not change the inward rectification (rectification index, 0·07 ± 0·01; $n = 6$). From these results, we concluded that inward rectification of P2X$_2$ was not caused by block of the channels by these extracellular negatively charged particles.

In summary, inward rectification of P2X$_2$ is unlikely to be due to block of channels at positive membrane potentials by charged impermeant ions.

Inward rectification is not caused by uneven distribution of permeant ions on the two sides of the membrane

P2X$_2$ is selectively permeable to cations, such as Na^+, K^+ and Ca^{2+} (Brake *et al.* 1994; Evans *et al.* 1996). The Goldman–Hodgkin–Katz current equation predicts inward rectification if the concentration of permeant cations is much higher outside than inside the cell (Goldman, 1943; Hodgkin & Katz, 1949). For our oocyte outside-out patch clamp recordings, the standard external solution was Na^+ rich and the standard internal solution was K^+ rich. To test whether this asymmetrical distribution of permeant ions contributes to inward rectification of P2X$_2$, a Na^+ solution which contained (mM): 150 NaCl, 1 $MgCl_2$, 10 Hepes and 10 EGTA (pH 7·4) was used as both the external and the internal solution in outside-out patch clamp recordings. Under these symmetrical conditions, the *I–V* relation still showed strong inward rectification when P2X$_2$ was expressed in patches drawn from oocytes (rectification index, 0·05 ± 0·01; $n = 9$) or HEK 293 cells (rectification index, 0·10 ± 0·03; $n = 9$). Similar results were obtained when patches were studied with a symmetrical K^+ solution, which contained (mM): 150 KCl, 10 Hepes, 1 $MgCl_2$ and 10 EGTA (pH 7·4) (rectification index, 0·05 ± 0·01; $n = 5$). Therefore, it was concluded that an uneven distribution of permeant ions on the two sides of the membrane was not the cause of inward rectification of P2X$_2$.

Voltage-dependent gating contributes to inward rectification of P2X$_2$

The hypothesis that voltage-dependent gating contributes to inward rectification predicts that P2X$_2$ channels will spend less time in the open state at positive membrane potentials. This hypothesis was evaluated by performing fast voltage

jump experiments (Adams, 1977) on patches expressing many receptors. Two protocols of voltage jumps were performed. The first protocol was to hold the patch at −100 mV and then jump the membrane potential to various more positive values (Fig. 2*A*). If voltage-dependent gating were the underlying cause of inward rectification of $P2X_2$, this protocol predicts that after fast voltage jumps, one should observe large instantaneous outward currents which then relax towards smaller steady-state currents with the closure of channels. Indeed this was the case. The second protocol was to hold the patch at +100 mV long enough to reach steady state, and then jump the membrane potential down to various more negative values (Fig. 2*B*). This protocol predicts that instantaneous inward currents should relax to much larger steady-state inward currents as channels reopen, and this too was observed. Results similar to those illustrated in Fig. 2 were found in all four patches tested.

Before we could quantitatively assess the results of voltage jump experiments we needed to take account of any effect of desensitization. The voltage jump protocols we used required a 1 s interpulse interval to allow the non-ATP dependent channels to return to their initial state between trials, and so an entire run required 5–10 s of continuous application of ATP. As noted above, the time constant of desensitization to 50 μM ATP observed in patches was 7·8 s and the steady-state level was 26% of the peak, so by the end of a 10 s exposure, the amplitude of ATP-activated currents was less than 50% of the initial value. The time constant of desensitization was very slow compared with the duration of our voltage steps (40–60 ms). For this reason, desensitization during each step would be expected to decrease the amplitude of currents by less than 1%, and so would have no effect on the time course of the relaxations observed, nor on the relative amplitude of the peak to steady-state currents at a single potential. However the

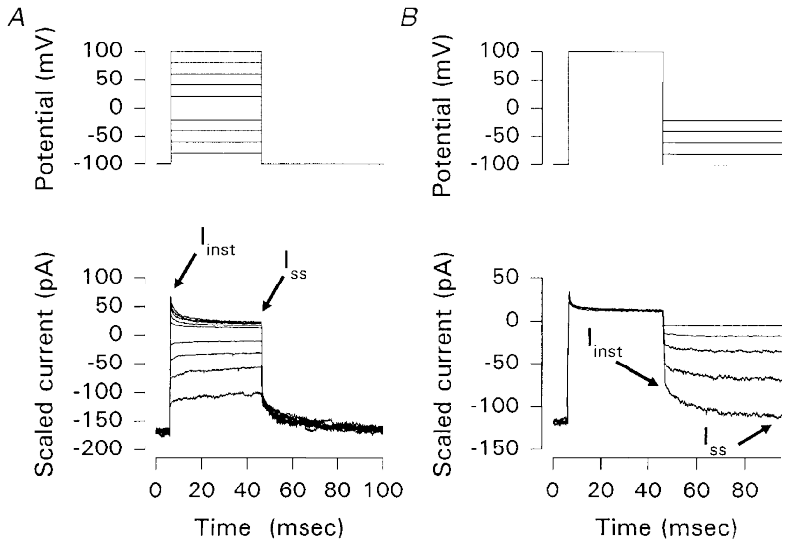

Figure 2. Voltage jump experiments on outside-out patches excised from oocytes expressing $P2X_2$

The patches were studied with standard external and internal solutions for oocyte patch clamp recordings. Because there was a considerable degree of desensitization (see Fig. 1*B*), the amplitudes of the currents illustrated in *A* and *B* were scaled so that all traces had the same initial amplitude at −100 mV. The amplitude scales represent the actual magnitude of the current during the first voltage step of each run. *A*, upward voltage jump protocol. Repetitive depolarizing voltage jumps were given to an outside-out patch. For each voltage jump, the patch was held at −100 mV and then the membrane potential was jumped to various more positive membrane potentials (from +100 to −80 mV, 20 mV apart) for 40 ms before it was stepped back to −100 mV. The interpulse interval was 1 s. Currents shown were recorded during application of 50 μM ATP after subtracting the capacity and leakage currents. I_{inst} (instantaneous current) was the current measured immediately after the upward voltage step and I_{ss} (steady-state current) was the current measured during the last 4 ms of the voltage step. *B*, downward voltage jump protocol. Repetitive voltage jumps were performed on an outside-out patch. For each voltage jump, the patch was held at −100 mV, the membrane potential was jumped to +100 mV and held there for 40 ms (long enough for the current to reach its steady state) and then the membrane potential was jumped to various more negative values (from −20 to −100 mV, 20 mV apart). The interpulse interval was 1 s. Currents shown were recorded during application of 50 μM ATP after subtracting the capacity and leakage currents. I_{inst} was the current measured immediately after the downward step, and I_{ss} was the current measured at the end of the trial.

desensitization occurring during the 1 s between pulses is significant enough (about 9%) that it must be taken into account before the complete *I–V* curve can be constructed. We compensated for desensitization by scaling each trial of a run up by a factor that made its amplitude at −100 mV just before the upward voltage step identical to the amplitude at −100 mV prior to the first voltage step of the run. The validity of this normalization procedure is supported by two lines of evidence. First, the protocol shown in Fig. 2*A* included a pulse to +100 mV at the beginning and the end of the run, and these two always superimposed when scaled up. Second, Fig. 2*B* illustrates that a series of steps from −100 to +100 mV all had identical time courses once the currents were scaled up, even though the last response was actually only 40% as large as the first response. We therefore conclude this simple normalization is an appropriate way to treat the data.

The normalized steady-state *I–V* relation (Fig. 3*A*) obtained from voltage jump experiments showed strong inward rectification (rectification index, 0·13 ± 0·02; $n = 4$), very similar to results obtained from voltage ramp experiments. The observation that there was no significant difference between steady-state rectification indices obtained from voltage ramp experiments and voltage jump experiments further confirmed that the voltage ramps used were slow enough for the currents to be in the steady state.

If voltage-dependent gating completely accounted for inward rectification, then the instantaneous *I–V* relation would be linear. However this was not the case (Fig. 3*A*). The normalized instantaneous *I–V* relation still showed substantial inward rectification (rectification index, 0·36 ± 0·09; $n = 4$). Comparison between the steady-state *I–V* relation and the instantaneous *I–V* relation showed that the difference between the instantaneous current (I_{inst}) and the steady-state current (I_{ss}) became much bigger at positive membrane potentials. This difference was more apparent when normalized instantaneous and steady-state conductances (Fig. 3*B*) were calculated from the corresponding *I–V* relations using the equation $g = I/(V_m - E_{rev})$, where g is the conductance, I is the current, V_m is the membrane potential and E_{rev} is the reversal potential, which under this recording condition was −5·4 mV. Both instantaneous and steady-state conductances decreased toward positive membrane potentials with steady-state conductance decreasing more rapidly. The time course of the relaxation of the instantaneous current to steady state could be fitted by a single exponential function and the time constant of the relaxation was sensitive to voltage (Fig. 3*C*). For 50 μM ATP the time constants at −100 and +100 mV were 12·2 ± 0·8 ms ($n = 6$) and 2·4 ± 0·3 ms ($n = 7$), respectively. As shown in Fig. 3*C*, the time constant decreased rapidly with membrane potential from −100 to −40 mV, while from −40 to

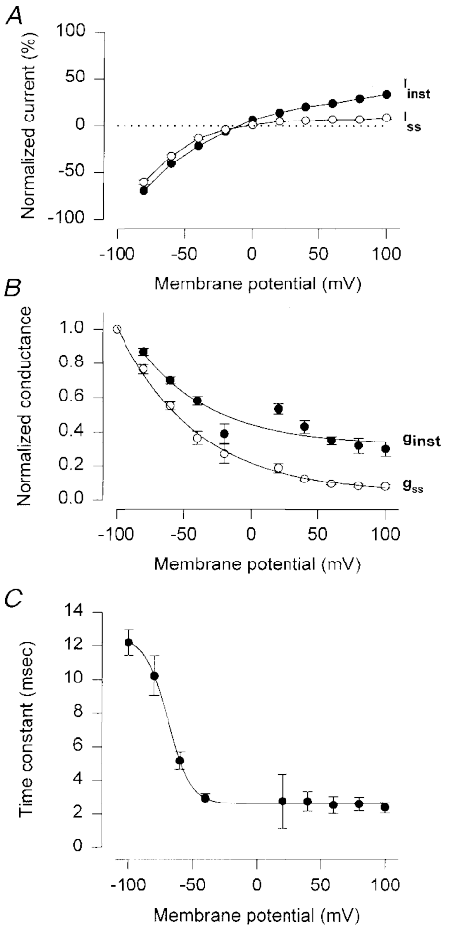

Figure 3. Voltage-dependent properties of $P2X_2$

A, *I–V* relations measured from voltage jump experiments on outside-out patches. For each jump, the instantaneous current (I_{inst}; ●) was the amplitude immediately after the jump and the steady-state current (I_{ss}; ○) was the amplitude during the last 4 ms of the jump (as illustrated in Fig. 2). Both currents were normalized to the holding current at −100 mV before each jump. Values are means ± S.E.M. ($n = 4$). Continuous lines are straight lines that connect adjacent points. *B*, normalized instantaneous conductance (g_{inst}, ●) and steady-state conductance (g_{ss}, ○) obtained from voltage jump experiments are plotted against membrane potential. This plot of normalized conductance (g) was calculated from the plot of normalized current (I) shown in Fig. 3*A* using the equation $g = I/(V_m - E_{rev})$, where $E_{rev} = -5{\cdot}4$ mV under these recording conditions. Conductance at different membrane potentials was normalized to the conductance at −100 mV before each voltage jump ($n = 4$). The continuous lines are single exponential fits to the data. *C*, the time constants of the current relaxations obtained from voltage jump experiments on outside-out patches in response to 50 μM ATP. Current relaxations at each membrane potential were fitted by single exponential functions ($n = 3$–7). The continuous line is a Boltzmann fit to the data. The data at −80, −60 and −40 mV were obtained from both of the protocols used in Fig. 3. The data at more positive potentials were obtained from the protocol shown in Fig. 2*A*.

+100 mV, the time constant became nearly voltage independent. For those potentials where the currents were large enough to measure with both of the protocols shown in Fig. 2 (−80, −60 and −40 mV), the time constant of the relaxation was the same using both protocols.

Inward rectification of $P2X_2$ is also due to a voltage dependence of the single channel conductance

The results of the voltage jump experiments indicated that voltage-dependent gating contributed to inward rectification of $P2X_2$. However, the observation that the instantaneous *I–V* relation was not linear suggested that a mechanism besides voltage-dependent gating must also contribute to inward rectification of $P2X_2$. Because open channel block and an imbalance of permeant ions had already been excluded as potential mechanisms, we evaluated whether the residual inward rectification present in the instantaneous *I–V* relation is caused by an intrinsic property of the channel. This hypothesis predicts that the single channel conductance would get smaller towards more positive membrane potentials, which would result in an inwardly rectifying single channel *I–V* relation.

To evaluate this hypothesis, single channel recordings were performed on outside-out patches excised from oocytes expressing $P2X_2$. In one set of experiments, membrane potential was held at a constant negative membrane potential and current responses to ATP were recorded. Unitary current was estimated from all points histograms and the single channel conductance was calculated (see Methods). Single channel conductances at −100 mV fell into two groups. Of twenty-seven patches studied in detail using 150 NaCl,

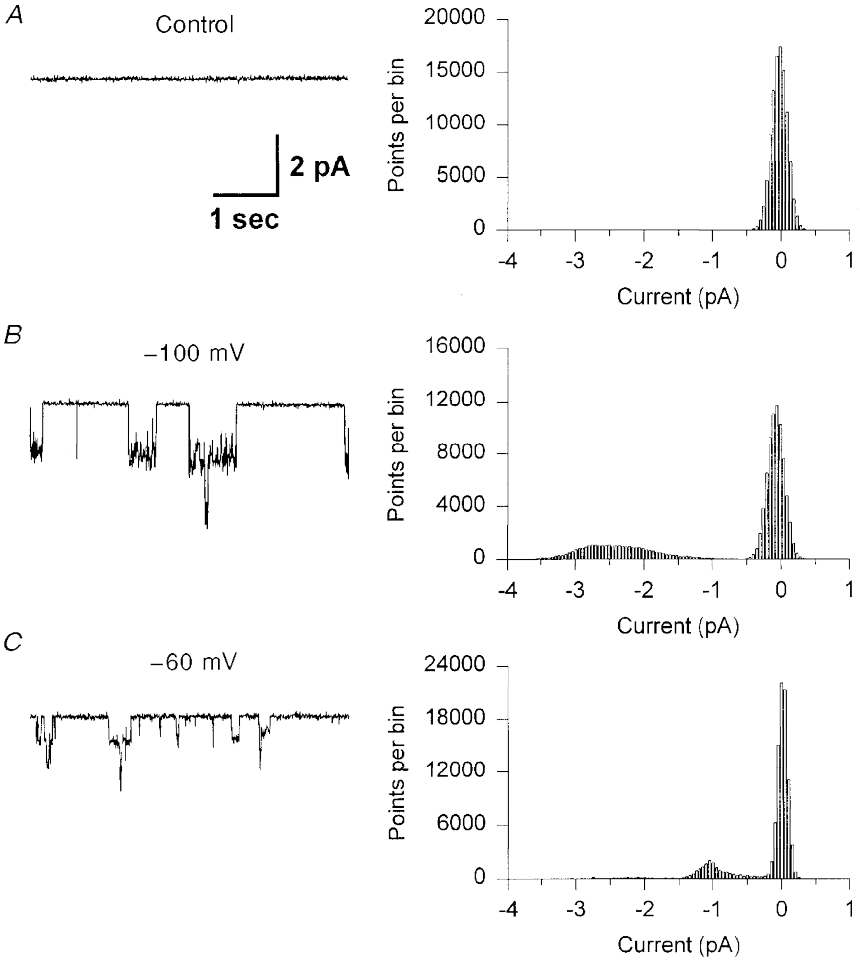

Figure 4. Single channel recordings from an outside-out patch excised from an oocyte expressing $P2X_2$

Current traces are shown to the left (the same scale is used for *A*, *B* and *C*) and all points histograms to the right. *A*, the patch was held at −100 mV in the absence of ATP. *B*, the same patch was held at −100 mV in the presence of 1 μM ATP. *C*, the same patch was held at −60 mV in the presence of 1 μM ATP. Unitary currents in the presence of ATP were estimated by fitting the all points histogram with the sum of two Guassian functions (one for the baseline, and one for single channel openings). A third peak, corresponding to two simultaneous openings had so few points that it did not appear above the baseline at the scale used in these figures, and made no significant contribution to the curve fits.

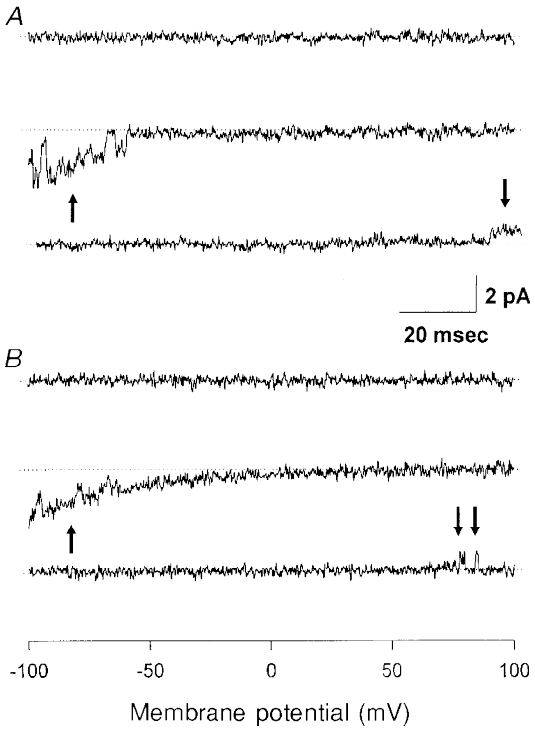

Figure 5. Single channel currents at different membrane potentials

Currents were obtained by applying series of 200 ms voltage ramps from −100 to +100 mV to outside-out patches excised from oocytes expressing $P2X_2$ in the presence and absence of 1 μM ATP. Traces obtained in the absence of ATP were subtracted from traces obtained in the presence of ATP to remove the leakage current. Because of the low agonist concentration, many traces obtained when ATP was present had no openings, and no traces showed two simultaneous openings. *A* and *B* are examples of current responses from two different patches. The same scale is used for *A* and *B*. The dotted line in each trace indicates the 0 current level. The arrows indicate periods during which channels were open.

1 $MgCl_2$, 10 Hepes (pH 7·4) and 10 EGTA as the solution on both sides of the patch, nineteen had a single class of openings of about 28 pS (Fig. 4*B*, mean single channel conductance for the nineteen patches was 27·6 ± 1·0 pS). The openings of these channels showed substantial flickering. In six patches there were openings to both the 28 pS level and to a smaller conductance level, and in two patches all openings went to the smaller level. Of these eight patches, five had enough openings at −100 mV to estimate the amplitude of the smaller channel class (14·5 ± 0·9 pS). When the patches that showed only the 28 pS class of openings at −100 mV were studied at −150, −120, −80, −60 and −40 mV, the single channel conductance showed a pronounced voltage dependence, with unitary conductances of 59·5 ± 2·9 ($n = 5$), 34·7 ± 0·2 ($n = 3$), 22·1 ± 0·7 ($n = 11$), 17·1 ± 0·6 ($n = 12$) and 13·8 ± 1·0 pS ($n = 7$), respectively. Three patches were studied in a solution containing no divalent cations (150 NaCl, 1 EDTA, 10 Hepes (pH 7·4), and 10 EGTA) bathing both sides of the patch. For these patches, the unitary conductance at −100 mV was 29·2 ± 1·5 pS and the unitary conductance at −60 mV was 16·9 ± 3·1 pS.

We were not able to obtain outside-out patches that were stable when maintained at positive membrane potentials for more than a few seconds, so in order to study single channel conductance at positive membrane potentials, we gave 200 ms ramp depolarizations from −100 to +100 mV in the presence and absence of ATP. Three important criteria had to be met before we accepted data from these experiments for analysis. First, the current responses recorded had to be from the openings of single channels rather than the simultaneous opening of two or more channels; to ensure this the concentration of ATP used was adjusted until many of the current traces recorded in the presence of ATP had no openings. Second, the openings at positive potentials had to represent ATP-activated channels, and therefore patches that showed channel openings at positive potentials in the absence of ATP (the majority studied) were excluded from further analysis. Third, because we wanted to study a uniform population of channels at different voltages, patches

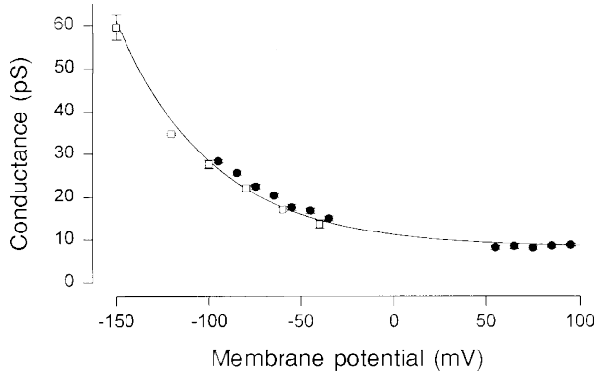

Figure 6. Single channel conductance decreased when membrane potential became more positive

Single channel conductances were calculated from single channel currents recorded during maintained recordings at a single potential (□) as illustrated in Fig. 4, or during ramp depolarizations (●) as illustrated in Fig. 5. The continuous line is the curve fitted to the plot of instantaneous conductance *versus* membrane potential (Fig. 3*B*), multiplied by a scaling factor that made the instantaneous conductance at −150 mV equal to 61 pS.

that showed the 14·5 pS class of openings at −100 mV were excluded from further analysis. Only five patches met all of these criteria. Figure 5 shows examples of individual traces from two of these patches. Because a low concentration of agonist was used, there were relatively few openings at each potential in each patch studied, but the results from all five patches were very similar, and so were averaged. Over the range of membrane potentials that was studied with both sustained recording at a single potential and with ramps, the estimates of single channel conductance at each potential were similar (Fig. 6). For instance, the portion of ramp data between −100 and −90 mV gave an estimated single channel conductance of $29{\cdot}3 \pm 0{\cdot}7$ pS ($n = 62$ openings) which closely matched the value of $27{\cdot}6 \pm 1{\cdot}0$ pS obtained by holding the membrane potential steady at −100 mV. The results of the ramp analysis indicated that single channel conductance continued to decrease at potentials more positive than those that could be studied with maintained depolarizations, but by +50 mV the conductance reached a level that did not decline much more with further depolarization. Over the range of +90 to +100 mV, the single channel conductance was estimated to be $9{\cdot}6 \pm 0{\cdot}3$ pS ($N = 87$ openings).

DISCUSSION

In the present study, we have investigated the mechanisms underlying inward rectification of $P2X_2$ when expressed in *Xenopus* oocytes and HEK 293 cells. Four possible mechanisms which are known to cause inward rectification of other ion channels were evaluated. We have concluded that inward rectification of $P2X_2$ is caused by dual mechanisms: voltage-dependent gating and voltage dependence of the single channel conductance.

In all outside-out patches studied, inward rectification was profound, with rectification ratios of 0·25 or less and little variation among cells or patches studied under similar experimental conditions. However, Evans *et al.* (1996) reported a large cell-to-cell variation in the degree of inward rectification of $P2X_2$ receptors expressed in HEK 293 cells and Chinese hamster ovary cells. Many of the cells they studied had rectification indices similar to those we obtained, but others showed rectification indices greater than 0·5. The difference between the two sets of results is not due to the use of two different rectification indices. Although in Results we report rectification indices for potentials 80 mV positive and negative to the reversal potential (to facilitate comparison with data generated on other channel types), in all cases we also calculated the rectification index for potentials 50 mV positive and negative to the reversal potential (as done by Evans *et al.*), and we never saw an example of a cell or patch in which this rectification index was greater than 0·5. The explanation for the discrepancy is unlikely to be the expression system used, since both studies used HEK 293 cells in some experiments. It should be noted that although we saw profound inward rectification in the steady-state *I–V* relation in all cells studied, the actual ratios obtained did show some variation between different experimental conditions. The mean rectification index obtained from studies of intact oocytes was 0·20, while the rectification indices obtained from experiments using whole-cell recording and outside-out patch recording ranged from 0·05 to 0·22. Although differences in ionic composition of solutions used in the various experiments probably contributed to the differences in rectification indices observed, it is possible that some of this variation might represent a less extreme version of the variation reported by Evans *et al.* (1996). One possible explanation for the variation in rectification indices is that there is some modulatory system that can put the $P2X_2$ channels into two distinct states, and that this system was nearly always in one state in our experiments, but varied between the two states in the experiments of Evans *et al.* (1996).

Intracellular polyamines are not required for inward rectification

Voltage-dependent block of ion channels by intracellular positively charged particles has been shown to be the mechanism of inward rectification of many ion channels. Recently, intracellular polyamines have been shown to cause inward rectification of native Ca^{2+}-permeable AMPA receptors. Since polyamines are found ubiquitously in both neuronal and non-neuronal cells (Shaw, 1979; Watanabe, Kusama-Eguchi, Kobayashi & Igarashi, 1991), one possibility we considered was that polyamines may have a general role as the cause of inward rectification in ligand-gated cation channels. Our results showed that inward rectification of $P2X_2$ was maintained in excised outside-out patches as long as patches could be held, even in the absence of intracellular polyamines. Furthermore, Mg^{2+} or polyamines at concentrations even greater than the physiological range did not have any effect on inward rectification of $P2X_2$. Therefore, unlike other intensively studied cation channels, inward rectification of $P2X_2$ is not caused by voltage-dependent block by these substances.

Dual mechanisms contribute to inward rectification of $P2X_2$

Voltage jump experiments revealed a substantial contribution of voltage-dependent gating to inward rectification of the steady-state *I–V* relation. However, the instantaneous *I–V* relation still showed considerable inward rectification, and so suggested that single channel conductance may decrease when membrane potential becomes more positive. This was confirmed by single channel recordings. Superimposing the curve fit to the normalized instantaneous conductance–voltage data (illustrated in Fig. 3*B*) onto the single channel conductance–voltage data (Fig. 6, continuous line) showed that the decrease in single channel conductance could quantitatively account for the inward rectification of the instantaneous *I–V* relation. Therefore, the combination of voltage-dependent gating and voltage dependence of the single channel conductance can quantitatively explain inward rectification of $P2X_2$. The voltage dependence of the single channel conductance causes instantaneous inward

rectification of P2X$_2$ with a rectification index of 0·36, while the voltage-dependent gating further shapes the *I–V* relation to be more inwardly rectifying in the steady state with a final steady-state rectification index of 0·13.

Inward rectification of neuronal nicotinic acetylcholine receptor currents in phaeochromocytoma (PC12) cells is caused by two voltage-dependent processes, block by Mg^{2+} and voltage-dependent gating (Ifune & Steinbach, 1990; Sands & Barish, 1992), with Mg^{2+} block dominant for fast events and voltage-dependent gating more important in the steady state. It has been suggested that the fast Mg^{2+} block is important for synaptic transmission, since when the membrane potential becomes more positive than the reversal potential for the nicotinic EPSP, the fast Mg^{2+} block will reduce acetylcholine-induced conductance rapidly and therefore ensure the fidelity of action potentials. Our results indicate that the temporal characteristics of inward rectification of P2X$_2$ are similar to those found in the neuronal nAChR channels in PC12 cells. Although the mechanism that causes the rapid inward rectification is different, both have one fast and one slow voltage-dependent mechanism to control rectification.

Why does the single channel conductance change with membrane potential?

Our single channel data indicated that the single channel conductance of P2X$_2$ decreases when the membrane potential becomes more positive. The mechanism underlying the single channel inward rectification is still unknown. One possibility is that rectification is simply intrinsic to the channel. It has been reported that a synthetic peptide, when inserted into an artificial membrane, forms a channel showing strong inward rectification (Kienker *et al.* 1994). This phenomenon was explained by a helical dipole model based on the alignment of amino acids which form the pore lining region of the channel. Therefore, the single channel rectification of P2X$_2$ could be due to the arrangement of amino acids lining the pore region. An alternative explanation is that some factor that we have not yet tested blocks the channel so rapidly that the time course of these transient blockages could not be resolved by our techniques. A very rapid block would be manifest as a decrease in mean conductance. Indeed, the fast flickering of channel openings observed in single channel recordings at −100 mV is consistent with this type of mechanism. Evans (1996) has also reported a rapid flickering of channel openings at −100 mV in P2X$_2$ channels expressed in Chinese hamster ovary cells, although this study reported a somewhat lower unitary conductance (21 pS) than we found for patches pulled from oocytes (28 pS). One possible explanation for the difference between the two studies is that the hypothetical blocker is at higher concentration in the solutions used by Evans (1996). Nakazawa & Hess (1993) reported that intracellular calcium or barium in the millimolar range can cause profound inward rectification in the *I–V* relation of the endogenous P2X receptor channels found in PC12 cells, and interpreted their data as indicating that these divalent cations act as voltage-dependent open channel blockers. These results seemed potentially relevant as P2X$_2$ messenger RNA is known to be highly expressed in PC12 cells (although the biochemical composition of the P2X channels of these cells is not yet known). Under physiological conditions, the only divalent cation present in the intracellular solution at millimolar levels is magnesium, a cation that was not tested by Nakazawa & Hess (1993). However, our experiments demonstrated that removing intracellular magnesium does not decrease inward rectification in the macroscopic or single channel *I–V* relations. Furthermore, Nakazawa & Hess (1993) found that the rapid flickering occurs even in the absence of divalent cations. For these reasons, we think that it is unlikely that block by divalent cations is a physiologically important mechanism that causes inward rectification in the single channel *I–V* relation of homomeric P2X$_2$ channels.

Implications of the present study

Inwardly rectifying whole-cell *I–V* relations of P2X receptors have been reported from intact neurons, including autonomic neurons from the rat superior cervical ganglion and guinea-pig coeliac ganglion (Evans, Derkach & Surprenant, 1992; Khakh, Humphrey & Surprenant, 1995), and sensory neurons from rat and bullfrog dorsal root ganglia (Bean, Williams & Ceelen, 1990). However, the mechanism underlying inward rectification of native P2X receptors is unknown. The subunit composition of native receptors is not clear at this point, although it has been suggested that the P2X receptors on one class of sensory neurons are formed by heteropolymerization of P2X$_2$ and P2X$_3$, since the pharmacological properties of ATP-gated currents in sensory neurons were mimicked by coexpression of P2X$_2$ and P2X$_3$ (Lewis, Neldhart, Holy, North, Buell & Surprenant, 1995). Both *in situ* hybridization and reverse trancriptase polymerase chain reaction studies indicate that P2X$_2$ messenger RNA is expressed in the rat brain (Kidd, Grahames, Simon, Michel, Barnard & Humphrey, 1995; Collo *et al.* 1996). Although it appears that some of the other P2X receptors are expressed more heavily in the brain than is P2X$_2$ (Collo *et al.* 1996), it still will be of great interest to determine whether any brain P2X receptors show the same mechanism of inward rectification as we have demonstrated for homomeric P2X$_2$ receptors, and if so, what effect this rectification has on neuronal signalling.

Adams, P. R. (1977). Relaxation experiments using bath-applied suberyldicholine. *Journal of Physiology* **268**, 271–289.

Bean, B. P., Willams, C. A. & Ceelen, P. W. (1990). ATP-activated channels in rat and bullfrog sensory neurons: current–voltage relation and single-channel behavior. *Journal of Neuroscience* **10**, 11–19.

Boulter, J., Hollmann, M., O'Shea-Greenfield, A., Hartley, M., Deneris, E., Maron, C. & Heinemann, S. (1990). Molecular cloning and functional expression of glutamate receptor subunit genes. *Science* **249**, 1033–1037.

Bowie, D. & Mayer, M. L. (1995). Inward rectification of both AMPA and kainate subtype glutamate receptors generated by polyamine-mediated ion channel block. *Neuron* **15**, 453–462.

Brake, A. J., Wagenbach, M. J. & Julius, D. (1994). New structural motif for ligand-gated ion channels defined by an ionotropic ATP receptor. *Nature* **371**, 519–523.

Buell, G., Collo, G. & Rassendren, F. (1996). P2X receptors: An emerging channel family. *European Journal of Neuroscience* **8**, 2221–2228.

Burnstock, G. (1995). Current state of purinoceptor research. *Pharmaceutica Acta Helvetiae* **69**, 231–242.

Chen, C. & Okayama, H. (1987). High-efficiency transformation of mammalian cells by plasmid DNA. *Molecular Cell Biology* **7**, 2745–2752.

Collo, G., North, R. A., Kawashima, E., Merio-Pich, E., Neidhart, S., Surprenant, A. & Buell, G. (1996). Cloning of $P2X_5$ and $P2X_6$ receptors and the distribution and properties of an extended family of ATP-gated ion channels. *Journal of Neuroscience* **16**, 2495–2507.

Davies, N. W., McKillen, H.-C., Stanfield, P. R. & Standen, N. B. (1996). A rate theory model for Mg^{2+} block of ATP-dependent potassium channels of rat skeletal muscle. *Journal of Physiology* **409**, 817–826.

Evans, R. J. (1996). Single channel properties of ATP-gated cation channels (P2X receptors) heterologously expressed in Chinese hamster ovary cells (CHO cells). *Neuroscience Letters* **212**, 212–214.

Evans, R. J., Derkach, V. & Surprenant, A. (1992). ATP mediates fast synaptic transmission in mammalian neurons. *Nature* **357**, 503–505.

Evans, R. J., Lewis, C., Virginio, C., Lundstrom, K., Buell, G., Surprenant, A. & North, R. A. (1996). Ionic permeability of, and divalent cation effects on, two ATP-gated cation channels (P_{2X} receptors) expressed in mammalian cells. *Journal of Physiology* **497**, 413–422.

Fakler, B., Brandle, U., Glowatzki, E., Weidemann, S., Zenner, H. P. & Ruppersberg, J. P. (1995). Strong voltage-dependent inward rectification of inward rectifier K^+ channels is caused by intracellular spermine. *Cell* **80**, 149–154.

Ficker, E., Taglialatela, M., Wible, B. A., Henley, C. M. & Brown, A. M. (1994). Spermine and spermidine as gating molecules for inward rectifier K^+ channels. *Science* **266**, 1068–1072.

Geetha-Habib, M., Park, H. R. & Lennarz, W. J. (1990). *In vivo* N-glycosylation and fate of Asn-X-Ser/Thr tripeptides. *Journal of Biological Chemistry* **265**, 13655–13660

Goldman, D. E. (1943). Potential, impedance, and rectification in membranes. *Journal of General Physiology* **27**, 37–61.

Hille, B. (1992). *Ionic Channels of Excitable Membranes.* Sinauer Associates Inc., Sunderland, MA, USA.

Hodgkin, A. L. & Katz, B. (1949). The effect of sodium ions on the electrical activity of the giant axon of the squid. *Journal of Physiology* **108**, 37–77.

Ifune, C. K. & Steinbach, H. (1990). Rectification of acetylcholine-elicited currents in PC12 pheochromocytoma cells. *Proceedings of the National Academy of Sciences of the USA* **87**, 4794–4798.

Kamboj, S. K., Swanson, G. T. & Cull-Candy, S. G. (1995). Intracellular spermine confers rectification on rat calcium-permeable AMPA and kainate receptors. *Journal of Physiology* **486**, 297–303.

Khakh, B. S., Humphrey, P. P. A. & Surprenant, A. (1995). Electrophysiological properties of P_{2X}-purinoceptors in rat superior cervical, nodose and guinea-pig coeliac neurones. *Journal of Physiology* **484**, 385–395.

Kidd, E. J., Grahames, C. B. A., Simon, J., Michel, A. D., Barnard, E. A. & Humphrey, P. P. A. (1995). Localization of P2X purinoceptor transcripts in the rat nervous system. *Molecular Pharmacology* **48**, 569–573.

Kienker, P. K., DeGrado, W. F. & Lear, J. D. (1994). A helical-dipole model describes the single-channel current rectification of an uncharged peptide ion channel. *Proceedings of the National Academy of Sciences of the USA* **91**, 4859–4863.

Koh, D. S., Burnashev, N. & Jonas, P. (1995). Block of native Ca^{2+}-permeable AMPA receptors in rat brain by intracellular polyamines generates double rectification. *Journal of Physiology* **486**, 305–312.

Lewis, C., Neldhart, S., Holy, C., North, R. A., Buell, G. & Surprenant, A. (1995). Coexpression of $P2X_2$ and $P2X_3$ receptor subunits can account for ATP-gated currents in sensory neurons. *Nature* **377**, 432–435.

Lopatin, A. N., Makhina, E. N. & Nichols, C. G. (1994). Potassium channel block by cytoplasmic polyamines as the mechanism of intrinsic rectification. *Nature* **372**, 366–369.

Magleby, K. L. & Stevens, C. F. (1972). A quantitative description of end-plate currents. *Journal of Physiology* **223**, 173–197.

Maricq, A. V., Peterson, A. S., Brake, A. J., Myers, R. M. & Julius, D. (1991). Primary structure and functional expression of the $5HT_3$ receptor, a serotonin-gated ion channel. *Science* **254**, 432–437.

Matsuda, H., Saigusa, A. & Irisawa, H. (1987). Ohmic conductance through the inwardly rectifying K channel and blocking by internal Mg^{2+}. *Nature* **325**, 156–159.

Methfessel, C., Witzemann, V., Takahashi, T., Mishina, M., Numa, S. & Sakmann, B. (1986). Patch clamp measurements on *Xenopus laevis* oocytes: currents through endogenous channels and implanted acetylcholine receptor and sodium channels. *Pflügers Archiv* **407**, 577–588.

Nakazawa, K. & Hess, P. (1993). Block by calcium of ATP-activated channels in pheochromocytoma cells. *Journal of General Physiology* **101**, 377–392.

Sands, S. B. & Barish, M. E. (1992). Neuronal nicotinic acetylcholine receptor currents in phaeochromocytoma (PC12) cells: Dual mechanisms of rectification. *Journal of Physiology* **447**, 467–487.

Sargent, P. B. (1993). The diversity of neuronal nicotinic acetylcholine receptors. *Annual Review of Neuroscience* **16**, 403–443.

Shaw, G. G. (1979). The polyamines in the central nervous system. *Biochemical Pharmacology* **28**, 1–6.

Vandenberg, C. A. (1987). Inward rectification of a potassium channel in cardiac ventricular cells depends on internal magnesium ions. *Proceedings of the National Academy of Sciences of the USA* **84**, 2560–2564.

Watanabe, S., Kusama-Eguchi, K., Kobayashi, H. & Igarashi, K. (1991). Estimation of polyamine binding to macromolecules and ATP in bovine lymphocytes and rat liver. *Journal of Biological Chemistry* **266**, 20803–20809.

Acknowledgements

We thank Dylan Clyne, Hui Liu, and Cheryl McCullum for helpful comments on this work. This research was supported by NIH grants NS 25782 and 33965.

Corresponding author

R. I. Hume: Department of Biology, University of Michigan, Natural Science Building, Ann Arbor, MI 48109-1048, USA.

Email: rhume@umich.edu